Astron. Astrophys. 352, 189–200 (1999)

ASTRONOMY AND ASTROPHYSICS

The photospheric filling factor of the active binary II Pegasi

G. Marino[1], **M. Rodonò**[1,2], **G. Leto**[2], **and G. Cutispoto**[2]

[1] Istituto di Astronomia, Università di Catania, Viale Andrea Doria 6, 95125 Catania, Italy
[2] Osservatorio Astrofisico di Catania, Viale Andrea Doria 6, 95125 Catania, Italy

Received 24 June 1999 / Accepted 12 October 1999

Abstract. UBV and JHK photometry of the active single-lined binary II Peg, we performed in 1995, is presented.

A method to determine the fraction of the photosphere covered by spots (filling factor) and to check the accuracy of generally assumed values of photospheric parameters has been developed. The procedure is based on the comparison between multiband fluxes and low resolution synthetic spectra weighted on the base of the spot filling factor and scaled with the ratio between the star radius and distance (R/d), so that we can also estimate the R/d ratio. A χ^2 fit has been performed for II Peg observations close to the light maximum and minimum by assuming reliable values of the photospheric parameters. Although a unique solution cannot be reached, we found clear indication for a spot filling factor at light maximum $\geq 40\%$. We find that the same set of parameters that gives us the best fit solutions at light maximum also provides the best fit at light minimum. The resulting solutions are consistent with the observed amplitude of the photometric wave, and with the commonly accepted value of R, unspotted V magnitude and spectral classification for II Pegasi.

Key words: stars: activity – stars: binaries: spectroscopic – stars: starspots – stars: individual: II Peg

1. Introduction

To explain the photometric variability of a large sample of late type stars, surface inhomogeneities are invoked. Several other features, such as the presence of C IV emission (Gunn et al. 1998), Ca II H & K (Montes et al. 1996), Mg II h & k (Pagano 1990; 1993; Byrne et al. 1998) and Hα lines (Bopp & Talcott 1978, 1980; Huenemoerder & Ramsey 1984; Liu & Tan 1986, Frasca & Catalano 1994), UV excesses (Amado & Byrne 1997), X-ray emission (Doyle et al. 1991, Griffiths & Jordan 1998), radio emission (Byrne et al. 1998) and flares (Doyle et al. 1989; Leto et al. 1997), lead to the conclusion that the photometric and spectroscopic behaviour of these active late type stars is due to the manifestation of solar type magnetic activity.

Send offprint requests to: G. Marino
Correspondence to: gmarino@alpha4.ct.astro.it

Most of the observational evidence requires photospheric and chromospheric structures much more enhanced than the ones observed on the Sun. Consequently, the existence of magnetic fields much stronger than solar are generally invoked.

To clarify the solar-stellar connection and to understand the origin of magnetic activity and its manifestation, it is necessary to know the physical and geometric parameters of activity features. Several observational and theoretical techniques exist to derive the temperature of unspotted and spotted areas and the absolute size of surface inhomogeneities, but they often depend very critically on some of the assumed parameters. Doppler-imaging techniques allow us to localise and map photospheric spots or chromospheric plages, but their absolute dimensions strongly depend on zero-point assumptions. The photometric spot-models of non-eclipsing binaries critically depend on the knowledge of the unspotted stellar flux (Rodonò et al. 1995, Lanza et al. 1998). In spectroscopy the absolute depth of TiO band constrains the cool spot's filling factor, while the ratio of their depths is a function only of the spot temperature (Neff et al. 1995), the results on the filling factors are strongly dependent on the assumed temperature of the unspotted photosphere. The best way to adopt reasonable assumption is to apply independent techniques to simultaneously obtained multiband data.

Multiband photometry can constrain the size and temperature of photospheric inhomogeneities, as shown by Vogt (1981b). He developed a method for the determination of starspot temperatures and areas for II Peg, BY Dra and HD 209813 from V and R light curves and using the Barnes-Evans surface brightness relation. A similar approach was followed by Poe & Eaton (1985) by using $UBVRI$ photometry. Both Vogt (1981b) and Poe & Eaton (1985) methods critically depend on the adopted value of the effective temperature and on the knowledge of the unspotted luminosity level. In their spot model of II Peg light curve, Byrne et al. (1995) used visual-infrared colours to constrain the temperature of spotted and unspotted area. Multiband photometry was associated with TiO spectroscopy by Neff et al. (1995) to determine a value of the unspotted temperature and then to derive appropriate values of the filling factor.

The present study is based on $UBVJHK$ photometry of II Peg collected in 1995. We show the results of a procedure for the determination of the spot filling factor and the best set of

photospheric parameters that are compatible with our photometry. To perform our study we have used low resolution synthetic spectra of cool stars by Hauschildt et al. (1999ab). These new models are based on molecular opacity data that have recently become available and include a detailed molecular equation of state.

1.1. II Pegasi

II Peg (=HD 224085) is a single-lined spectroscopic binary classified as K2-3 IV-III by Rucinski (1977). Its optical variability was first discovered by Chugainov (1976), who interpreted it as due to the rotational modulation of photospheric spots. The photometric and orbital period (~ 6.72d) are very close, showing that the system is tidally locked. Wave-like light curves with peak-to-peak V-band amplitudes up to 0.5 magnitude have been reported (Byrne 1986, Cutispoto et al. 1987). A detailed study of the stellar and orbital parameters was done by Berdyugina et al. (1998a).

II Peg has been observed by using several techniques in a wide range of wavelengths.

Several photometric studies are available: e.g., Vogt 1981b; Poe & Eaton 1985; Rodonó et al. (1986), Rodonó & Cutispoto 1992; Mohin & Raveendran 1993; Byrne at al. 1995; Henry et al. 1995. Vogt (1981ab) and Poe & Eaton (1985) argue that it is not possible to interpret the observed modulation as due to hot spots; only cool inhomogeneities have to be invoked.

Optical spectroscopy has been performed, for instance, by Hatzes (1995), Frasca & Catalano (1994), Byrne et al. (1995), Byrne at al. (1998). They studied also the correlations between photospheric and chromospheric activity. Doppler imaging was obtained by Hatzes (1995) and Berdyugina et al. (1998b, 1999) by analysing a sample of appropriate photospheric lines.

Rodonò et al. (1987) found the UV emission line fluxes, observed with the IUE satellite, to vary in anti-phase with the optical variations; they interpreted these results as evidence of a close spatial correlation between spot and plage-like features.

Recently, TiO band spectroscopy by Neff et al. (1995) and O'Neal et al. (1998a) seems to confirm that, even at the historic light maximum, the II Peg photosphere was covered by a amount of cool spots having a total area of about 35% of the visible hemisphere.

II Peg was observed by IRAS (Busso et al. 1988) and ISO spacecraft (Rodonò et al. 1997), the latter observations showing very clear evidence of IR excess. Near and intermediate infrared excesses were also found by Lazaro (1988) and Scaltriti et al. (1993a), who attributed them to circumstellar matter.

Radio interferometry has been performed by Gunn et al. (1994) to determine the physical parameters of radio emission regions, and radio flares were detected by van den Oord & de Bruyn (1994). Moreover, II Peg is one of the few RS CVn stars for which optical flares have been detected (Henry & Newsom 1996, Byrne et al. 1995).

Rodonò & Cutispoto (1992) pointed out that, in addition to the long-term variability discovered from Harvard plates (Hartmann et al. 1979), short-term variability of the mean magnitude on time scales of less than 10 years suggests a solar-type magnetic cycle. An extensive study on magnetic cycles in four active binaries including II Peg was performed by Henry at al. (1995). II Peg is included in a systematic long-term monitoring programme of active stars and systems carried out at Catania Observatory since the early 90's with an APT-80 telescope (Rodonò & Cutispoto 1994).

2. Observations

2.1. UBV photometry

UBV photometry has been performed with the 80-cm APT at the *M. G. Fracastoro* station of Catania Astrophysical Observatory (Mt. Etna, Italy) and with the 25-cm Phoenix APT on Mt. Hopkins (AZ, USA).

Both the Catania and Phoenix APTs feed a single-channel photometer equipped with uncooled Hamamatzu R1414 and 1P21 photomultipliers, respectively and standard filters matching the UBV system. The observations were made differentially with respect to the nearby comparison and check stars HD 224016 and HD 223461, respectively. The typical precision of the differential photometry is of the order of 0.015, 0.010 and 0.007 magnitudes for U, B and V, respectively. Further details can be found in Rodonò & Cutispoto (1992) and in Strassmeier et al. (1997).

2.2. IR photometry

JHK photometry was performed by using the 91-cm Cassegrain telescope of the *M. G. Fracastoro* station of Catania Astrophysical Observatory feeding an InSb photometer based on a single InSb diode cooled with liquid nitrogen and equipped with interference JHK filters. The resulting photometric system (Leto 1990) matches the Johnson-Glass system (Johnson 1965, 1966; Glass 1974) described by Koornneef (1983). Background emission has been subtracted by using a chopper system oscillating at 10 Hz. The integration times were 9–10 s for the variable, comparison and check stars and about 1 s for the brightest standard stars.

The comparison star adopted for II Peg was HD 222842. For such a bright star the signal–to–noise ratio is high enough that the typical error on acquired data is smaller than 0.02 magnitudes. The stability of the comparison star was monitored by observing HD 224427 as check star.

The standard deviations of differential JHK magnitudes are in the range 0.02-0.03 magnitude.

In order to reduce our photometry to the standard system, we observed a sample of standard stars from Koornneef (1983) and Johnson et al. (1966). The empirical formulae in the Koornneef paper were used to calculate the H magnitudes that were not present in the Johnson et al. (1966) list. This calibration was performed during the same nights when the atmospheric extinction coefficients were measured.

The obtained standard magnitude of the comparison star HD 222842 are: $J = 3.40 \pm 0.05$, $H = 2.89 \pm 0.03$, and $K = 2.78 \pm 0.02$.

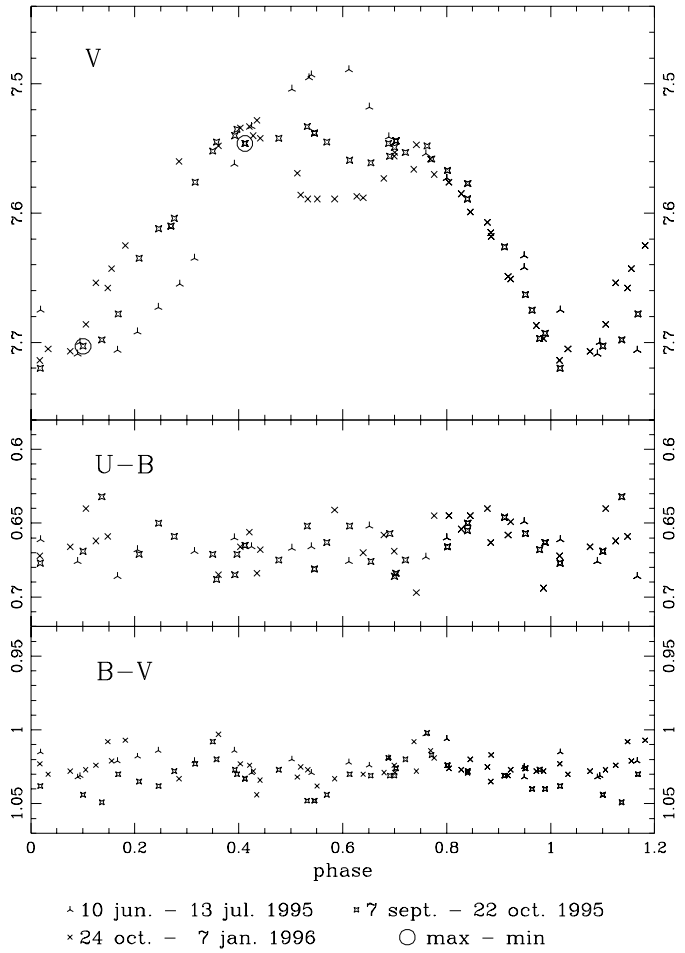

Fig. 1. UBV light curves of II Peg from 1995, June 10 to 1996, January 7. *Open circles* indicate the data used for the analysis of multiband photometry (see text).

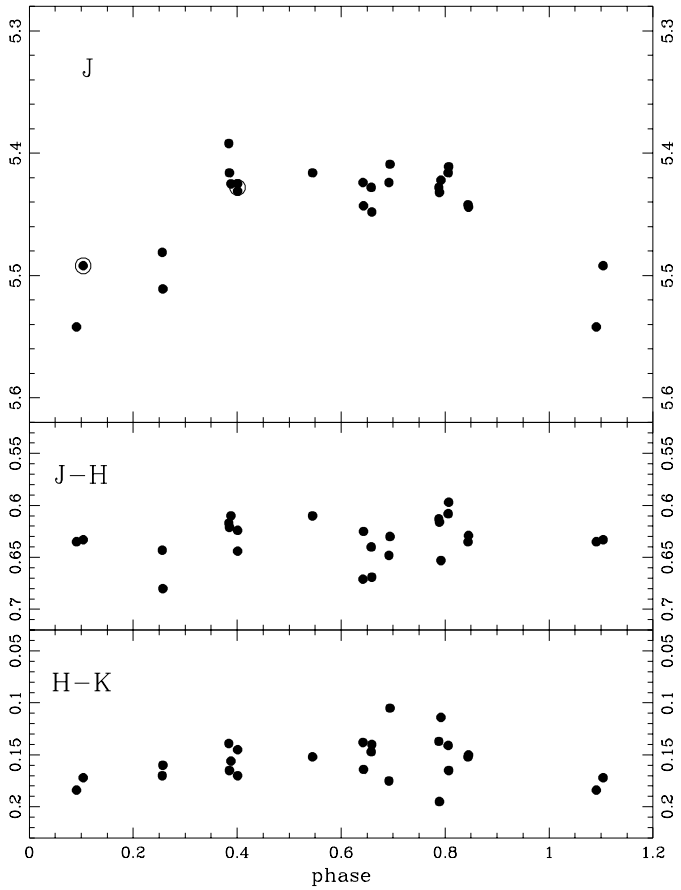

Fig. 2. J light curve, and $J-H$ and $H-K$ colour curves of II Peg from 1995, August 26 to September 22. *Open circles* are the data we used for the analysis of multiband photometry (see text).

3. Light curves of II Peg in 1995

Fig. 1 and 2 show the UBV and JHK light curves, respectively. Phases are reckoned from the spectroscopic ephemeris (Rucinski 1977):

$$HJD = 2443033.10 + 6.724183E.$$

The well known enhanced and variable character of II Peg activity is evident in the visual light curve where, in particular, the depression of the light maximum, that occurred within a few months after 1995 July, suggests the appearance of a new extended spotted region. The amplitude of the V-band wave decreased from about 0.22 up to about 0.16 magnitude. There is no clear modulation of the $U-B$ and $B-V$ colours, while a clear wave-like variation of the $B-V$ colour was present, for instance, in 1988 and 1989 (Rodonò & Cutispoto 1992). The light maximum is rather faint with respect to other epochs, as it is possible to see by comparing our data with those collected by Henry et al. (1995). This suggests the presence of a widely extended longitude distribution of cool spots, which do not produce a large amplitude "wave" and any evident modulation of the colour indexes.

In addition to UBV modulation also the IR curve shows a photometric wave as already found by Lazaro et al. (1987), but with a smaller amplitude than in UBV, consistently with a modulation of brightness due to the presence of cool spots. The scatter in the IR curve may be attributed not only to measure uncertainties, but also to intrinsic variations of the photospheric active region distribution at the epoch of the observations. Also the IR band fluxes are lower than in previous years (Lazaro et al. 1987; Marino 1994).

4. Modelling of colours from near UV to near IR

We have developed a method to estimate the absolute value of the spot filling factor in a single-lined spotted star and, at the same time, to check which values of the photospheric parameters are the most reliable. Moreover, we can obtain a new estimate of the R/d ratio and therefore, of the radius by using the distance given by HIPPARCOS.

Our procedure is based on finding the atmosphere model and the filling factor which best reproduce the observed spectral distribution given by multiband photometry from near UV to near IR. The various steps of our method are described below.

Table 1. Magnitudes of II Peg close to light maximum and minimum in 1995

	U	B	V	J	H	K
close to light max.	9.24	8.58	7.55	5.43	4.79	4.64
close to light min.	9.42	8.75	7.70	5.49	4.86	4.69
	$\pm$0.03	0.02	0.02	0.06	0.06	0.06

4.1. Data selection

The data set on which our analysis is based has been selected according to the following criteria:

- the multiband data have been collected nearly simultaneously;
- the data are representative of the light curve maximum and minimum.

The second item is important in order to be able to verify whether there is a relevant spot filling at maximum and to test that the results are consistent with the amplitude of the observed photometric wave. For the light maximum we have chosen the photometric data on JD 2449968, when II Peg was observed in UBV and JHK bands during the same night. The corresponding magnitudes are plotted as large open circles in the light curves of Figs. 1 and 2. These data also satisfy the second criterion over an interval of several months. Moreover, at that phase the system luminosity was almost constant throughout the whole period of observations.

Close to the light minimum we do not have contemporary observations. Hence, we have chosen the UBV data of Julian Day 2450006 and the JHK data of Julian Day 2449966. These data are distant in observing dates but, they may well represent the situation at light minimum, because our UBV light curves indicate that at that phase the magnitude was almost constant during the time interval of our observations. These points are identified by large open circles on the light curves in Fig. 1 and 2.

The adopted magnitudes at light maximum and minimum are listed in Table 1.

4.2. Synthetic flux in the photometric bands

To analyse the spectral distribution inferred from our multiband photometry we have adopted low resolution spectra synthesised with the Phoenix code (Hauschildt et al. 1999ab). Phoenix is a code specially developed for cool stars. The synthetic spectra we used were produced by these authors with the NextGen photosphere models, (code V. 5.0).

To calculate the synthetic fluxes in the different photometric bands we have applied the normalised response curves (see Johnson 1965, Ažusienis & Straižys 1966, Bessel 1983, Bessel 1986, Alonso et al. 1994) to the model low resolution spectra and scaled to the values of zero magnitude given by Busso et al. (1988) and Bell & Gustafsson (1989). The atmospheric passbands of Manduca & Bell (1979) were also taken into account.

4.3. Modelling observed magnitudes

We have performed several fits of the magnitudes given in Table 1 with synthetic spectra simulating the emission of unspotted and spotted areas of II Peg. The flux at Earth is given by:

$$F = (\frac{R}{d})^2[(1-f)F_u + fF_s] \quad (1)$$

where f is the filling factor, and F_u and F_s are the flux of unspotted and spotted areas, respectively. The synthetic spectra have been weighted with filling factor and scaled by means of the $(R/d)^2$ ratio. To determine the best combination of the filling factor and the R/d ratio, we searched for the minimum χ^2 solution.

The typical accuracy of the reduction to the standard system have been calculated by propagating standard deviations on coefficients and zero–points, the latter being the main source of uncertainty. The resulting accuracy of absolute photometry is about 0.03 magnitude on U, 0.02 magnitude on B and V, 0.06 magnitude on J, H and K. However, to search for model solutions, and to easily reach convergence, we have assumed typical accuracy about 30% larger than the above values.

5. Results and discussion

The photospheric parameters of II Peg have been determined by several authors, in spite of the difficulties due to the presence of enhanced and variable activity. Vogt (1981b) gave a temperature for spots (T_s) of 3400 K, similar to that of Poe & Eaton (1985). Byrne at al. (1995) found values of T_s between 2600 and 3600 K, similar to that found by Huenemoerder & Ramsey (1987), while Mohin & Raveendran (1993) derived a T_s greater than 3700 K. Neff et al (1995) found a temperature for unspotted region $T_u \approx 4800$ K and T_s equal to 3500 K, the last being similar to the value given by Berdyugina et al. (1998b). Berdyugina et al. (1998a) found a $T_{\rm eff}$ of about 4600 K. O'Neal et al. (1998b) found evidence for multiple spot temperature between 3350 K and 3550 K.

On the base of these determinations, we have explored the two fit parameters, filling factor and R/d ratio, over a grid of T_u, T_s, $\log g$ and metallicity values, which include the values in the literature. To obtain acceptable fits it was necessary to introduce a correction δU of the theoretical U-band flux to take into account the $U-B$ excess discussed by Amado & Byrne (1997) for active stars. A correction δB with different values of B has been tested, as Amado (1997) has shown the presence of an excess also in the $B-V$ index in his sample of active stars. The δU and δB values were chosen within the range suggested in the above quoted references.

Tables 2a–f contain the numerical results of our fits. Under "Activity Factor" we give the excess applied to correct for activity effects. There are only few combinations of photospheric parameters which allow us to get acceptable fits, i.e. χ^2 values smaller that about 1.0 implying associated probabilities of more than 35%. The hypothesis that the filling factor is zero is ruled out by our fits because the associated reduced χ^2 are as high as 10 or more, leading to negligible probabilities.

Table 2a. Results of reduced χ^2 fits to multiwavelength photometry of II Peg in 1995. Data in bold characters are the reduced χ^2 values (4 freedom degrees) for the cases with associated probability greater than 35%.

unspotted area $T_u = 4800$ K		*spotted area* $T_s = 3500$ K		"Activity Factors"		*AT LIGHT MAX.*			*AT LIGHT MIN.*		
$\log g$	$[M/H]$	$\log g$	$[M/H]$	δU	δB	χ^2	% spots	R/d factor	χ^2	% spots	R/d factor
4.0	0.0	4.0	0.0	0.30	0.00	**0.60**	52.7	0.845	**0.42**	59.9	0.843
					0.10	1.21	55.1	0.851	1.16	62.0	0.849
				0.25	0.00	**1.13**	51.3	0.840	**0.89**	58.8	0.833
					0.10	2.23	53.8	0.846	2.14	61.0	0.845
				0.10	0.00	5.39	47.7	0.828	5.02	55.8	0.828
					0.10	7.78	51.0	0.837	7.58	58.6	0.836
				0.00	0.00	10.17	45.8	0.822	9.72	54.3	0.823
					0.10	13.24	49.5	0.832	12.98	57.1	0.830
	-0.5		-0.5	0.30	0.00	3.13	67.6	0.926	2.74	72.8	0.922
					0.10	1.79	69.0	0.930	1.50	74.0	0.927
				0.25	0.00	2.11	65.6	0.910	1.81	71.0	0.908
					0.10	**1.02**	67.5	0.921	**0.84**	72.7	0.917
				0.10	0.00	**0.40**	61.0	0.889	**0.88**	67.3	0.887
					0.10	1.44	63.3	0.897	1.51	69.2	0.895
				0.00	0.00	1.90	57.2	0.867	2.11	64.3	0.868
					0.10	4.72	60.0	0.877	5.05	66.5	0.876
3.5	0.0	3.5	0.0	0.30	0.00	19.0	72.7	0.915	19.22	76.2	0.901
					0.10	15.8	73.4	0.916	16.20	76.8	0.901
				0.25	0.00	19.5	71.3	0.908	19.88	75.0	0.894
					0.10	16.3	72.1	0.909	16.80	75.6	0.893
				0.10	0.00	7.3	67.9	0.896	7.64	72.0	0.882
					0.10	6.67	69.0	0.897	7.20	72.9	0.882
				0.00	0.00	2.61	65.8	0.889	2.92	70.1	0.875
					0.10	3.73	67.1	0.890	4.24	71.2	0.875
	-0.5		-0.5	0.30	0.00	**0.66**	54.2	0.838	**0.64**	61.9	0.841
					0.10	2.76	57.1	0.847	2.79	64.2	0.849
				0.25	0.00	**0.82**	52.5	0.831	**0.80**	60.4	0.834
					0.10	4.14	54.8	0.834	4.57	62.4	0.837
				0.10	0.00	4.86	46.4	0.804	4.97	55.6	0.810
					0.10	10.6	50.7	0.817	10.8	59.0	0.821
				0.00	0.00	10.2	43.5	0.793	10.31	53.4	0.801
					0.10	17.1	48.6	0.809	17.39	57.5	0.815

With $T_u = 4800$ K and $T_s = 3500$ K (Neff at al. 1995) there are only six cases with probability associated to χ^2 (in boldface in Table 2a) greater than 35%. In two cases the filling factor at light maximum is between 61% and 67% and was obtained by assuming $\log g = 4$ and $[M/H] = -0.5$. The other four best solutions indicate filling factor of about 53% for $\log g = 4$ and $[M/H] = 0$, and $\log g = 3.5$ and $[M/H] = -0.5$, respectively. Estimated errors in the filling factors are of about $\pm 4\%$ and were determined in all cases by considering the shape of χ^2, following Press et al. (1992).

Also for $T_u = 4800$ K and $T_s = 3400$ K (Table 2c) there are two groups of solutions. By assuming $\log g = 4$ and $[M/H] = -0.5$ we find one acceptable solution with a spot filling factor of about 62% at maximum brightness, while four acceptable solutions with resulting filling factor between about 54% and 56%.

For $T_u = 4600$ K and $T_s = 3500$ K (Table 2b), as well as for $T_u = 4600$ K and $T_s = 3400$ K (Table 2d) we find acceptable solutions for filling factors equal to 48.1% and 50.0%, respectively.

Since a value of $\log g = 3.2$ has been also determined for II Peg (Berdyugina et al. 1998a), our calculation for $\log g = 4.0$ and $\log g = 3.5$ were extended to $\log g = 3.0$ (Tables 2e and 2f). In this case the synthetic spectra (some of these purposely computed for us by Dr. Peter H. Hauschildt) include spherical symmetry (Hauschildt et al. 1999b). Due to the limited availability of atmosphere models, we considered $T_s = 3400$ K and 3600 K bracketing the $T_s = 3400$ K and 3500 K we used for the other models.

For $\log g = 3$ and the same previously considered parameters, besides the same two groups solutions (filling factor at light maximum $f_{max} \approx 53\%$ and $\approx 64\%$) we find four acceptable fits with $f_{max} \approx 40\%$. Such relatively small value of the filling factor, was obtained for $T_u = 4600$ K (both for $T_s = 3600$ K and for $T_s = 3400$ K) but not for $T_u = 4800$ K that gives solutions with rather large filling factors.

Table 2b. (as Table 2a)

unspotted area $T_u = 4600$ K		*spotted area* $T_s = 3500$ K		"Activity Factors"		*AT LIGHT MAX.*			*AT LIGHT MIN.*		
$\log g$	$[M/H]$	$\log g$	$[M/H]$	δU	δB	χ^2	% spots	R/d factor	χ^2	% spots	R/d factor
4.0	0.0	4.0	0.0	0.30	0.00	8.27	15.3	0.782	7.50	29.9	0.790
					0.10	9.35	20.9	0.793	8.75	34.5	0.800
				0.25	0.00	13.4	11.4	0.770	9.97	26.9	0.779
					0.10	38.2	13.3	0.733	11.50	33.3	0.797
				0.10	0.00	25.5	8.0	0.763	19.10	26.1	0.782
					0.10	28.3	14.7	0.776	21.35	31.1	0.792
				0.00	0.00	35.1	6.1	0.760	26.34	24.7	0.779
					0.10	38.2	13.3	0.733	28.92	30.2	0.790
	-0.5		-0.5	0.30	0.00	6.23	10.1	0.758	6.10	28.4	0.777
					0.10	8.20	17.9	0.775	8.12	34.7	0.794
				0.25	0.00	13.7	7.5	0.756	8.37	26.3	0.771
					0.10	15.7	16.0	0.775	10.76	33.1	0.789
				0.10	0.00	25.7	1.7	0.743	17.06	21.2	0.757
					0.10	28.7	11.8	0.765	20.32	29.4	0.778
				0.00	0.00	35.2	1.0	0.743	24.07	18.6	0.750
					0.10	38.6	9.5	0.759	27.75	27.7	0.773
3.5	0.0	3.5	0.0	0.30	0.00	3.58	53.4	0.883	3.71	59.5	0.871
					0.10	2.45	55.0	0.885	2.72	60.8	0.872
				0.25	0.00	2.31	51.5	0.876	2.04	58.1	0.867
					0.10	1.64	53.1	0.877	1.65	59.7	0.869
				0.10	0.00	**0.32**	48.1	0.871	**0.21**	54.7	0.859
					0.10	1.58	49.6	0.869	1.52	56.6	0.861
				0.00	0.00	1.86	45.0	0.861	1.52	52.7	0.854
					0.10	4.66	47.5	0.864	3.83	54.9	0.857
	-0.5		-0.5	0.30	0.00	1.69	17.6	0.766	1.61	33.3	0.780
					0.10	4.49	26.6	0.782	6.48	38.5	0.793
				0.25	0.00	3.40	12.1	0.749	2.90	31.1	0.774
					0.10	7.78	19.7	0.765	6.28	36.8	0.788
				0.10	0.00	11.6	10	0.75	9.12	25.3	0.758
					0.10	17.5	13.7	0.75	13.79	32.4	0.775
				0.00	0.00	19.0	0.00	0.722	14.91	22.5	0.751
					0.10	25.9	10.7	0.743	20.23	30.0	0.768

From a simple inspection of the results of our calculations that are collected in Table 2 it is possible to note that, though for a) $T_u = 4600$ K, $T_s = 3500$ K and 3400 K, $\log g = 3.5$ and $[M/H] = -0.5$ and b) for $T_u = 4600$ K, $T_s = 3600$ K and 3400 K, $\log g = 3.0$ and $[M/H] = 0.0$, good fits are not obtained (i.e., the associated probability is in the range 16-18%), it is remarkable that χ^2 decreases towards greater δU "activity factors". These cases are interesting because they seem to lead to values of the spot filling factor $\sim$ 20% - 30% at light maximum. However, also for the very active star II Peg, Amado & Byrne (1997) and Amado (1997) did not consider the δU values greater than 0.30 to be realistic. Since Amado (1997) suggests that a large UV excess should be associated to a relevant B-band excess, we consider more realistic the solutions obtained for $\delta U = 0.30$ and $\delta B > 0$, i.e. those listed in Table 2e with filling factors 31.2 and 33.4% ($T_u = 4600$ K, $T_s = 3600$ K and 3400 K, $\log g = 3.0$ and $[M/H] = 0.0$).

To summarise, three groups of acceptable solutions with probability $\geq 35\%$ were found:

I) $f_{max} \approx 40\%$: four cases for $T_u = 4600$ K, $\log g = 3.0$ and $[M/H] = -0.5$;

II) f_{max} from $\approx 47\%$ up to $\approx 57\%$: fifteen cases with different atmosphere models among those we considered;

III) $f_{max} \approx 64\%$: six solutions for $T_u = 4800$ K and different combinations of T_s, $\log g$ and $[M/H]$

and two other groups of possible solutions with probability in the range 18-16%:

I') $f_{max} \approx 20\%$: two cases for $T_u = 4600$ K, $\log g$=3.0 and $[M/H]$=0.0 (all of them obtained for $\delta U = 0.30$ and $\delta B = 0.0$);

II') $f_{max} \approx 32\%$: three cases for $T_u = 4600$ K, $\log g$=3.0 and $[M/H]$=0.0 (tw of them obtained for $\delta U = 0.30$ and $\delta B = 0.10$).

Fig. 3 shows the fluxes at $UBVJHK$ bands in the proximity of the light maximum of II Peg superimposed to the synthetic spectrum which was obtained by weighting and scaling the models for $T_u = 4600$ K, $T_s = 3400$ K, $\log g = 3.5$, $[M/H] = 0$,

Table 2c. (as Table 2a)

unspotted area $T_u = 4800$ K		*spotted area* $T_s = 3400$ K		"Activity Factors"		*AT LIGHT MAX.*			*AT LIGHT MIN.*		
$\log g$	$[M/H]$	$\log g$	$[M/H]$	δU	δB	χ^2	% spots	R/d factor	χ^2	% spots	R/d factor
4.0	0.0	4.0	0.0	0.30	0.00	**0.62**	54.9	0.868	**0.44**	62.19	0.870
					0.10	1.19	57.3	0.876	1.11	64.0	0.877
				0.25	0.00	**1.11**	53.6	0.863	**0.87**	60.9	0.865
					0.10	2.43	55.5	0.866	2.05	63.1	0.873
				0.10	0.00	6.40	49.3	0.844	4.90	58.2	0.854
					0.10	9.53	52.5	0.854	7.40	60.7	0.862
				0.00	0.00	12.6	47.2	0.836	9.56	56.7	0.848
					0.10	16.6	51.1	0.849	12.76	59.5	0.857
	-0.5		-0.5	0.30	0.00	3.64	68.4	0.948	3.35	73.4	0.949
					0.10	2.27	69.8	0.954	2.06	74.5	0.950
				0.25	0.00	2.55	66.3	0.932	1.87	72.2	0.938
					0.10	1.60	68.0	0.940	1.20	73.4	0.942
				0.10	0.00	**0.15**	61.7	0.905	**0.29**	68.3	0.911
					0.10	1.54	63.9	0.914	1.40	70.1	0.919
				0.00	0.00	1.61	58.6	0.888	1.52	66.0	0.897
					0.10	4.42	61.5	0.900	3.72	68.2	0.907
3.5	0.0	3.5	0.0	0.30	0.00	19.8	74.1	0.946	20.2	77.4	0.932
					0.10	16.5	74.7	0.946	17.0	77.9	0.931
				0.25	0.00	20.4	72.8	0.938	15.9	76.5	0.928
					0.10	12.9	73.7	0.942	13.4	77.1	0.928
				0.10	0.00	5.94	69.8	0.928	6.22	73.6	0.914
					0.10	5.29	70.8	0.929	5.67	74.6	0.917
				0.00	0.00	2.20	67.9	0.921	2.42	71.9	0.907
					0.10	2.88	69.1	0.923	3.21	73.0	0.909
	-0.5		-0.5	0.30	0.00	**0.75**	56.1	0.860	**0.73**	63.7	0.867
					0.10	2.80	59.1	0.872	2.84	66.1	0.878
				0.25	0.00	**0.84**	53.5	0.845	**0.82**	62.3	0.860
					0.10	3.51	57.7	0.865	3.54	65.0	0.872
				0.10	0.00	3.88	50.1	0.834	3.83	58.7	0.842
					0.10	8.20	54.2	0.849	8.23	62.1	0.856
				0.00	0.00	7.95	47.5	0.823	7.88	56.6	0.832
					0.10	13.2	52.2	0.840	13.2	60.5	0.848

with a filling factor of 50%. The spectrum plotted in Fig. 3 has been degraded to 50 Å resolution.

In Fig. 4 the distribution of minimum reduced χ^2 values corresponding to our fits with $T_u = 4600$ K and $T_s = 3400$ K is shown. The plot shows that the fit reliability and its constraints are rather good, in fact the χ^2 increases quite rapidly crossing the χ^2 minimum.

As expected, we did not find any clear constraint on the spot temperature within reasonable values, because the contribution of the spotted areas is very low with respect to the emission from the quiet photosphere.

In Table 2 the second parameter of the fits, the R/d ratio, is also given. It is expressed in terms of $R = 3.4 R_\odot$ (Berdyugina et al. 1998a) and $d = 42.3^{+1.7}_{-1.5}$ pc from the HIPPARCOS Catalogue (Perryman et al. 1997). The best fits values of R/d ratio are smaller than 1, this may indicate a radius smaller than 3.4 $R_\odot$, as discussed below.

Fig. 5 is the same as Fig. 3 for the observations performed in the proximity of the light minimum. In this case ($T_u = 4600$ K, $T_s = 3400$ K, $\log g = 3.5$) the filling factor is 56.6%, $[M/H] = 0$. This solution is similar to that obtained with $T_u = 4600$ K, $T_s = 3500$ K, $\log g = 3.5$.

We note that the best fit solutions at light minimum were found with the same set stellar parameters as at light maximum. The best R/d values for light maximum and minimum are very similar and the best filling factors at light minimum are consistent with the values obtained for the light maximum. In fact, given a configuration of spotted areas on the photosphere, the ratio between the surface stellar flux at light minimum (F_{min}) and maximum (F_{max}) in the V-band is given by:

$$\frac{F_{min}}{F_{max}} = \frac{(1 - f_{min})F_u + f_{min}F_s}{(1 - f_{max})F_u + f_{max}F_s} \quad (2)$$

where f_{max} and f_{min} are the filling factors, and F_u and F_s the V-band surface fluxes of the unspotted and spotted areas, respectively.

From Eq. 2 we have

Table 2d. (as Table 2a)

unspotted area $T_u = 4600$ K		*spotted area* $T_s = 3400$ K		"Activity Factors"		*AT LIGHT MAX.*			*AT LIGHT MIN.*		
$\log g$	$[M/H]$	$\log g$	$[M/H]$	δU	δB	χ^2	% spots	R/d factor	χ^2	% spots	R/d factor
4.0	0.0	4.0	0.0	0.30	0.00	8.25	16.7	0.789	7.47	31.9	0.803
					0.10	9.32	22.7	0.803	8.69	36.4	0.814
				0.25	0.00	10.8	15.0	0.785	9.91	30.7	0.800
					0.10	12.1	21.2	0.799	11.4	35.5	0.812
				0.10	0.00	20.1	11.6	0.778	19.0	27.9	0.793
					0.10	22.1	18.5	0.793	21.3	33.2	0.806
				0.00	0.00	27.4	10.1	0.775	26.3	26.6	0.790
					0.10	29.7	17.5	0.795	28.8	32.3	0.804
	-0.5		-0.5	0.30	0.00	6.19	10.9	0.762	5.95	29.8	0.787
					0.10	8.14	19.6	0.784	7.97	36.1	0.806
				0.25	0.00	8.50	10.1	0.762	8.23	27.8	0.781
					0.10	10.8	17.5	0.778	10.6	34.6	0.801
				0.10	0.00	17.3	1.5	0.739	16.9	23.0	0.767
					0.10	20.4	12.6	0.765	20.2	30.9	0.785
				0.00	0.00	24.3	0.0	0.737	23.9	20.8	0.761
					0.10	27.8	10.6	0.760	27.6	29.3	0.784
3.5	0.0	3.5	0.0	0.30	0.00	4.53	49.7	0.859	3.92	61.2	0.895
					0.10	2.50	56.9	0.908	2.80	61.9	0.891
				0.25	0.00	2.06	54.0	0.902	2.17	60.0	0.892
					0.10	1.41	55.7	0.905	1.64	61.5	0.894
				0.10	0.00	**0.28**	50.0	0.888	**0.17**	56.6	0.882
					0.10	1.30	52.2	0.895	1.34	58.5	0.889
				0.00	0.00	1.63	47.9	0.886	1.38	54.6	0.876
					0.10	3.62	50.3	0.890	3.55	56.8	0.880
	-0.5		-0.5	0.30	0.00	1.67	19.2	0.774	1.55	35.3	0.794
					0.10	4.44	26.5	0.793	4.39	40.7	0.810
				0.25	0.00	2.99	16.2	0.766	2.82	33.3	0.788
					0.10	6.24	24.1	0.786	6.17	39.0	0.804
				0.10	0.00	9.23	8.9	0.748	9.01	27.7	0.771
					0.10	13.8	18.4	0.770	13.63	34.7	0.790
				0.00	0.00	15.1	4.8	0.738	14.79	24.8	0.763
					0.10	20.2	15.7	0.763	20.07	31.7	0.779

$$f_{min} = \frac{\frac{F_{min}}{F_{max}} \cdot (1 - f_{max}) - 1 + \frac{F_{min}}{F_{max}} \cdot f_{max} \frac{F_s}{F_u}}{\frac{F_s}{F_u} - 1} \quad (3)$$

Then, from our observations where $\Delta V = 0.16$, considering for instance $T_u = 4600$ K, $T_s = 3400$ K, $\log g = 3.5$ and $[M/H] = 0.0$, with $f_{max} = 50.0\% \pm 4\%$ we find, from Eq. 3, $f_{min} = 57.2 \pm 4\%$. For $T_u = 4600$ K, $T_s = 3500$ K, $\log g = 3.5$ and $[M/H] = 0.0$, with $f_{max} = 48.1\% \pm 4\%$ we find $f_{min} = 55.8 \pm 4\%$. Both set of parameters lead to maximum filling factors that within the data uncertainty are quite consistent with those presented before. Consistent results are also obtained for the other groups of solutions.

In order to evaluate the filling factor variation from the maximum up to the minimum light we computed the spot coverage corresponding to each plotted point of the September – October 1995 V light curve (this light curve represents the mean behaviour of II Peg during our observations). In Fig. 6 this variation is shown for the case of filling factor of 50% at V=7.55, i.e., close to the light brightest magnitude of II Peg.

The brightest observed magnitude of II Peg was V=7.28 (Cutispoto et al. 1989). We used Eq. 3 to check the consistency of all our solutions previously discussed (see Table 3). We find that four out of the five solution groups lead to a residual spot coverage at the light maximum ever observed (7.28 mag) ranging from 13 to 49%. The other group of solutions with 19% filling factor at light maximum implies a -6% spot coverage, that means that some excess flux must be considered, e.g., the presence of bright spots.

We have further inspected the five classes of solutions evaluating the V unspotted immaculate magnitude. The results are given in Table 4. For the solutions of the type II we find a V_{unsp}=6.84, really close to the value (6.9 mag) obtained by Berdyugina et al. 1998a, with a different approach based on the analysis of the TiO bands.

If the possibility of a large fraction of spotted area is considered, small variations of the filling factor are enough to account for the light curves variations. Therefore, the small variations of $V - R$ and $V - I$ discussed by Poe & Eaton (1985) would

Table 2e. (as Table 2a)

unspotted area		*spotted area*									
$T_u = 4600$ K		$T_s = 3600$ K		"Activity Factors"		*AT LIGHT MAX.*			*AT LIGHT MIN.*		
$\log g$	$[M/H]$	$\log g$	$[M/H]$	δU	δB	χ^2	% spots	R/d factor	χ^2	% spots	R/d factor
3.0	0.0	3.0	0.0	0.30	0.00	1.74	27.9	0.806	1.43	38.7	0.803
					0.10	1.42	31.2	0.811	1.27	41.4	0.807
				0.25	0.00	2.55	26.0	0.802	2.22	37.0	0.799
					0.10	2.67	29.5	0.807	2.50	39.9	0.803
				0.10	0.00	7.55	20.5	0.790	7.12	32.5	0.788
					0.10	8.79	25.0	0.797	8.55	36.1	0.794
				0.00	0.00	12.7	17.7	0.784	12.2	30.2	0.783
					0.10	14.5	22.6	0.792	14.2	34.1	0.789
	-0.5		-0.5	0.30	0.00	3.69	47.3	0.862	3.24	55.6	0.858
					0.10	1.69	49.2	0.865	1.40	57.0	0.859
				0.25	0.00	2.22	44.6	0.853	1.89	53.4	0.850
					0.10	**0.77**	46.7	0.856	**0.60**	55.0	0.851
				0.10	0.00	**0.53**	36.8	0.829	**0.49**	46.5	0.825
					0.10	**0.74**	39.8	0.834	**0.86**	49.0	0.829
				0.00	0.00	1.65	33.0	0.820	1.73	42.4	0.812
					0.10	2.86	35.6	0.821	3.12	45.4	0.817
$T_u = 4600$ K		$T_u = 3400$ K									
3.0	0.0	3.0	0.0	0.30	0.00	1.54	30.1	0.823	1.16	40.8	0.825
					0.10	1.18	33.4	0.830	0.92	43.4	0.830
				0.25	0.00	2.30	28.1	0.818	1.83	39.3	0.821
					0.10	2.36	31.8	0.826	2.04	42.2	0.827
				0.10	0.00	7.19	23.6	0.808	6.50	35.4	0.811
					0.10	8.35	28.0	0.817	7.85	39.0	0.819
				0.00	0.00	12.3	21.3	0.803	11.5	33.4	0.806
					0.10	14.0	25.9	0.812	13.4	37.4	0.815
	-0.5		-0.5	0.30	0.00	4.52	50.1	0.896	4.29	58.2	0.898
					0.10	2.48	51.9	0.900	2.37	59.6	0.901
				0.25	0.00	2.78	47.6	0.886	2.58	56.0	0.888
					0.10	1.30	49.8	0.891	1.24	57.9	0.893
				0.10	0.00	**0.51**	40.3	0.859	**0.40**	50.2	0.864
					0.10	**0.69**	43.3	0.866	**0.73**	52.6	0.870
				0.00	0.00	1.40	35.7	0.843	1.32	46.6	0.850
					0.10	2.58	39.4	0.852	2.66	49.5	0.857

not be in contrast with a large filling factor, because the colour variation amplitude is smoothed out.

Accounting for the U-band excess due to enhanced activity on II Peg, our study shows that it is possible to find reasonable photospheric parameters without introducing IR excesses in the observed JHK magnitudes.

Among the five different solution classes, the type II is characterised by high probability and it is also consistent with the V unspotted magnitude given in literature. This class of solutions also leads to the largest number of acceptable solutions (15), while the other classes give between two and six possible solutions.

To obtain an estimate of the spectral type and radius of II Peg from our data we start by considering that the $U-B$ and $B-V$ colours are consistent with those of an evolved K2 active star. The absolute magnitude of a K2 V star is $M_v = 6.37$ (Houk et al. 1997), its effective temperature is $T_{\rm eff} = 4984$ K (Flower 1996) and its radius is $R = 0.8 R_\odot$ (Straižys & Kuriliene 1981). By adopting the HIPPARCOS distance, the absolute magnitude of II Peg, corresponding to the unspotted level of $V = 6.84 \pm 0.06$ (our type II solution), is $M_v = 3.70^{+0.15}_{-0.16}$ i.e. much brighter than for a K2 V star. By scaling for a $T_{\rm eff} = 4600$ K and taking into account the value of M_v we find $R = 3.1^{+0.2}_{-0.3}\ R_\odot$. This is consistent with the best fit R/d factor obtained with $T_u = 4600$ K and $T_s = 3400$ K, which leads to $R = 3.02 \pm 0.15 R_\odot$. These estimate of the absolute magnitude and radius lead to K2 IV for the spectral classification of II Peg.

For $R = 3.1^{+0.2}_{-0.3}\ R_\odot$ we find an inclination of the rotation axis to the line of sight (i) of $\approx 75^\circ$, equal to the value by Scaltriti et al. (1993b) from linear polarisation measures.

From the type II solution class, we have obtained R, V unspotted and spectral type that are in good agreement with other recent determinations obtained with a different method (see Berdyugina et al. 1998a). Our results are also fully con-

Table 2f. (as Table 2a)

unspotted area		*spotted area*									
$T_u = 4800$ K		$T_s = 3600$ K		"Activity Factors"		*AT LIGHT MAX.*			*AT LIGHT MIN.*		
$\log g$	$[M/H]$	$\log g$	$[M/H]$	δU	δB	χ^2	% spots	R/d factor	χ^2	% spots	R/d factor
3.0	0.0	3.0	0.0	0.30	0.00	3.37	59.1	0.855	3.20	64.9	0.847
					0.10	1.80	60.5	0.857	1.76	66.1	0.848
				0.25	0.00	1.87	57.5	0.829	1.72	63.5	0.841
					0.10	**0.87**	59.1	0.852	**0.86**	64.8	0.843
				0.10	0.00	**0.36**	52.9	0.833	**0.25**	59.4	0.825
					0.10	**1.01**	55.0	0.837	**1.06**	61.3	0.829
				0.00	0.00	1.74	50.0	0.823	1.64	57.1	0.817
					0.10	3.39	52.7	0.829	3.45	59.4	0.822
	-0.5		-0.5	0.30	0.00	13.9	72.4	0.925	12.6	76.5	0.915
					0.10	10.2	73.0	0.925	9.08	77.0	0.914
				0.25	0.00	10.7	70.8	0.916	9.64	75.1	0.906
					0.10	7.60	71.5	0.916	6.70	75.7	0.905
				0.10	0.00	3.61	65.8	0.890	3.07	70.8	0.881
					0.10	2.29	67.0	0.892	1.92	71.8	0.882
				0.00	0.00	**1.00**	62.5	0.874	**0.75**	67.9	0.865
					0.10	**0.89**	64.0	0.876	**0.82**	69.2	0.867
$T_u = 4800$ K		$T_s = 3400$ K									
3.0	0.0	3.0	0.0	0.30	0.00	4.36	60.3	0.882	4.49	65.9	0.876
					0.10	2.70	61.8	0.886	2.92	67.1	0.879
				0.25	0.00	2.52	58.8	0.876	2.59	64.7	0.871
					0.10	1.44	60.5	0.881	1.61	66.0	0.875
				0.10	0.00	**0.22**	54.9	0.862	**0.12**	61.3	0.858
					0.10	**0.80**	56.9	0.867	**0.83**	63.1	0.863
				0.00	0.00	1.23	52.6	0.854	1.01	59.2	0.850
					0.10	2.81	54.9	0.860	2.75	61.3	0.856
	-0.5		-0.5	0.30	0.00	17.7	74.3	0.979	16.9	77.9	0.968
					0.10	13.8	74.5	0.979	13.3	77.9	0.960
				0.25	0.00	13.9	72.8	0.968	13.4	75.9	0.948
					0.10	10.6	73.6	0.970	10.1	77.5	0.963
				0.10	0.00	5.23	68.5	0.942	4.92	73.2	0.937
					0.10	3.81	69.5	0.943	3.64	74.1	0.939
				0.00	0.00	1.80	65.5	0.924	1.67	70.7	0.921
					0.10	1.65	66.9	0.928	1.64	71.9	0.924

sistent with those obtained by Vogt (1981a), Huenemoerder & Ramsey (1987) and Neff et al. (1995) based on the analysis of TiO band. They found that the values of filling factor due to cool spot on II Peg is always greater than about 35%. Similar results were found by O'Neal & Neff (1997) from the OH absorption excess. Surface images of II Peg by Hatzes (1995) and Berdyugina et al. (1998b) lead to variation of the filling factor between 10 and 15% that is not in contrast with our estimate of slightly less than 10%.

Table 3. Spot filling factors at the V=7.28 historic maximum of II Peg (Cutispoto et al. 1989) obtained by assuming different spot coverage value at V=7.55 (close to our assumed light maximum), for the five solution classes discussed (I': 19.2%, II': 33.4%, I:40.3%, II: 50.0%, III: 61.7%). The uncertainties of tabulated filling factor are of $\pm 4\%$.

	I'	II'	I	II	III
V=7.28	(-6%)[a]	13%	21%	34%	49%

[a] This value implies the presence of hot spot.

6. Conclusions

We have developed a photometric method to evaluate the projected area covered by spots and to test the photospheric parameters of spotted stars. The method is based on contemporary multiband photometry and low resolution synthetic spectra. We have applied our method to $UBVJHK$ photometry of II Peg performed in 1995 and, taking into account excess in U-band. Although a unique solution cannot be obtained, we find clear indication for a spot filling factor at light maximum $\geq 40\%$, in agreement with some previous determinations.

Our fits cannot exclude the possibility of filling factors in the range 20-30%, but a filling factor as small as 20% is not in agreement with the observed historic maximum.

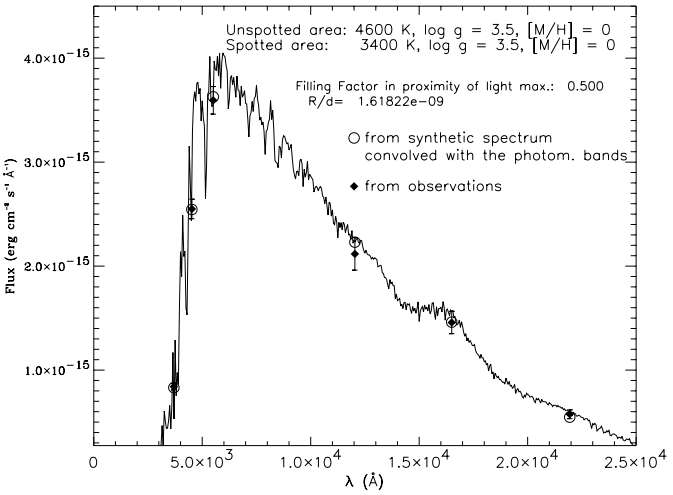

Fig. 3. Observed fluxes close to the II Peg light maximum (full points) and synthetic low resolution spectrum (thin line) obtained for a filling factor of 50.0% and using the atmosphere models of Hauschildt et al. (1999a). This is the best-fit value of the filling factor that was obtained by adopting the atmosphere model parameters indicated at the figure top. The synthetic spectrum has been degraded to 50 Å resolution.

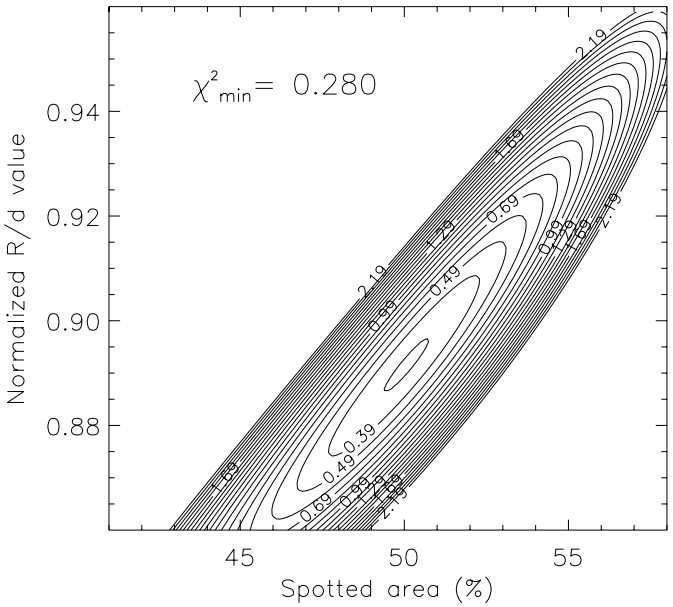

Fig. 4. Minimum value of reduced χ^2 fit to the multiband photometry of II Peg at light maximum in Fig. 3.

The estimated radius $R = 3.1^{+0.2}_{-0.3}\ R_{\odot}$, the V_{unsp}, the spectral type, together with other parameters such as temperatures of spotted and unspotted regions, for our type II solutions, are in substantial agreement with previous determinations and lead to an inclination of the rotation axis in the range from $60°$ to $75°$.

Acknowledgements. The authors wish to thank A.F. Lanza, F. Leone and P.J. Amado for suggestions and useful discussions since the begin of the present work. GM is also grateful to P.H. Hauschildt for kindly computing and making available to us detailed synthetic spectra. We also thank the referee, S. Berdyugina, for the stimulating comments.

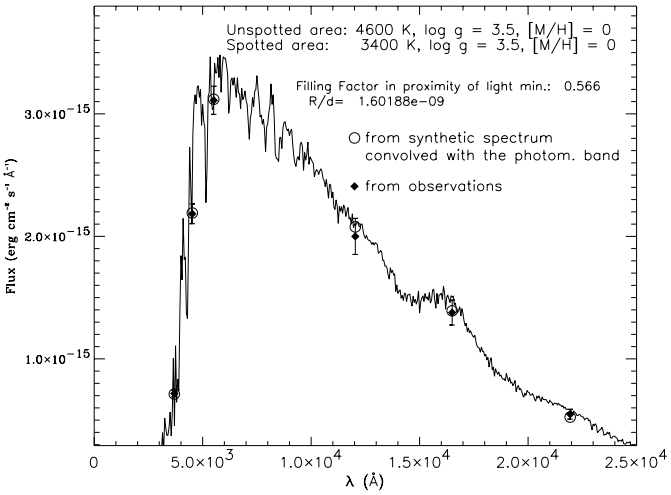

Fig. 5. As Fig. 3, for observations close to the II Peg light minimum.

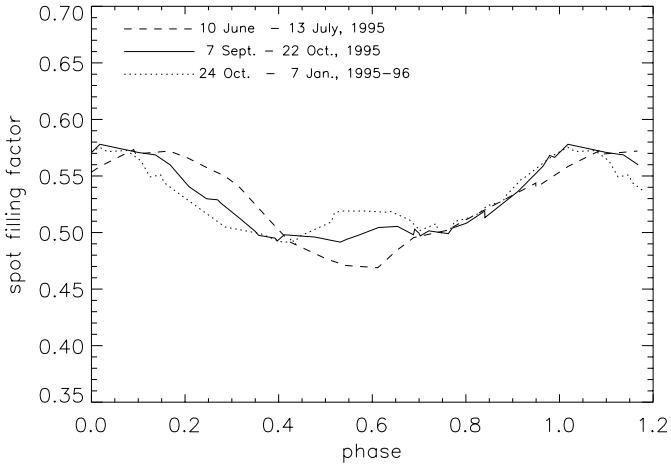

Fig. 6. Spot filling factors for II Peg in three consecutive epochs. The best system and model parameters that were derived from the present study were adopted.

Table 4. Expected unspotted V magnitude (V_{unsp}) obtained by assuming different spot coverage values at V=7.55 (close to assumed light maximum), for the five classes of solution we discuss in the text. The uncertainties on V_{unsp} are of ± 0.06 mag.

% spot coverage at V=7.55	19.2	33.4	40.3	50.0	61.7
V_{unsp}	7.34	7.13	7.04	6.84	6.62

Stellar activity research at Catania Observatory is supported by the Italian *Ministero dell' Università e della Ricerca Scientifica e Tecnologica*, and by the *Regione Sicilia*, through research grants that are gratefully acknowledged.

References

Alonso A., Arribas S., Martínez-Roger C., 1994, A&AS 107, 365
Amado P.J., 1997, Ph.D. Thesis, Queen's Univ. of Belfast
Amado P.J., Byrne P.B., 1997, A&A 319, 967
Ažusienis A., Straižys V., 1966, Bull. Vilnius Astron. Obs. 16, 3; 17, 3

Bell R.A., Gustafsson B., 1989, MNRAS 236, 653
Berdyugina S.V., Jankov S., Ilyin I., et al., 1998a, A&A 334, 863
Berdyugina S.V., Berdyugin A.V., Ilyin I., et al., 1998b, A&A 340, 437
Berdyugina S.V., Berdyugin A.V., Ilyin I., Touminen I., 1999, A&A in press
Bessel M.S., 1983, PASP 95, 480
Bessel M.S., 1986, PASP 98, 354
Byrne P.B., 1986, IBVS, No. 2951
Byrne P.B., Panagi P.M., Lanzafame A.C., et al., 1995, A&A 299, 115
Byrne P.B., Abdul Aziz H., Amado P.J., et al., 1998, A&AS 127, 505
Bopp B.W., Talcott J.C., 1978, AJ 83, 1517
Bopp B.W., Talcott J.C., 1980, AJ 85, 55
Busso M., Scaltriti F., Persi P., et al., 1988, MNRAS 234, 445
Chugainov P.F., 1976, Izv. Krymsk. Ap. Obs. 54, 89
Cutispoto G., Leto G., Pagano I., et al., 1987, IBVS, No. 3034
Cutispoto G., Leto G., Pagano I., 1989, IBVS, No. 3379
Doyle J.G., Butler C. J., Byrne P.B., et al., 1989, A&A 223, 219
Doyle J.G., Kellet B.J., Butler C.J., et al., 1991, MNRAS 248, 503
Flower P.J., 1996, ApJ 469, 355
Frasca A., Catalano S., 1994, A&A 284, 883
Glass I.S., 1974, MNRAS 33, 53 and 71 (erratum)
Griffiths N.W., Jordan C., 1998, ApJ 497,883
Gunn A.G., Mitrou C.K., Doyle J.G., 1998, MNRAS 296,150
Gunn A.G., Spencer R.E., Abdul Aziz H., et al., 1994, A&A 291, 847
Hartmann L., Londoño C., Phillips M.J., 1979, ApJ 229, 183
Hatzes A., 1995, In: Strassmeier K.G. (ed.) Poster Proceedings Stellar Surface Structure. IAU Symp. 176, Univ. Vienna, p. 87
Hauschildt P., Allard F., Baron E., 1999a, ApJ 512, 377
Hauschildt P., Allard F., Ferguson J., Baron E., Alexander D.R., 1999b, ApJ in press
Henry G.W., Eaton J.A., Hamer J., Hall D.S., 1995, ApJS 97, 513
Henry G.W., Newsom M.S., 1996, PASP 108, 242
Houk N., Swift C.M., Murray C.A., et al., 1997, In: Proceedings: HIPPARCOS Venice 97 Symposium, ESA SP–402, p. 279
Huenemoerder D.P., Ramsey L.W., 1984, AJ 89, 549
Huenemoerder D.P., Ramsey L.W., 1987, ApJ 319, 392
Johnson H.L., 1966, ARA&A 4, 193
Johnson H.L., 1965, ApJ 141, 925
Johnson H.L., Mitchell R.I., Iriarte B., et al., 1966, Comm Lunar & Planetary Lab. 4, 99
Koornneef J., 1983, A&AS 51, 489
Lanza A.F., Catalano S., Cutispoto G., et al., 1998, A&A 332, 541
Lázaro C., Arévalo M.J., Fuensalida J.J., 1987, Ap&SS 134, 347
Lázaro C., 1988, A&A 193, 95
Leto G., 1990, Laurea Thesis, Univ. of Catania
Leto G., Pagano I., Rodonò M., et al., 1997, A&A 327, 1114
Liu X., Tan H., 1986, Chin. Astron. Astrophys. 10, 221
Manduca A., Bell R.A., 1979, PASP 91, 848
Marino G., 1994, Laurea Thesis, Univ. of Catania
Mohin S., Raveendran A.V., 1993, A&A 277, 155
Montes D., Fernańdez-Figueroa M.J., Cornide M., et al., 1996, A&A 312, 221
Neff J.E., O'Neal D., Saar S.H., 1995, ApJ 452, 879
O'Neal D., Neff J.E., 1997, AJ 113, 1129
O'Neal D., Neff J.E., Saar S.H., 1998a, ApJ 507, 919
O'Neal D., Saar S.H., Neff J.E., 1998b, ApJ 501L, 730
Pagano I., 1990, Laurea Thesis, Univ. of Catania
Pagano I., 1993, Ph.D. Thesis, Univ. of Catania
Poe C.H., Eaton J.A., 1985, ApJ 289, 644
Perryman M.A.C., Lindegren L., Kovalevsky J., et al., 1997, A&A 323, L49
Press W.H., Teukolsky S.A., Vetterling W.T., et al., 1992, Numerical Recipies. Cambridge University Press, p. 687
Rodonò M., Byrne P.B., Neff J.E., et al., 1987, A&A 176, 267
Rodonò M., Cutispoto G., Pazzani V., et al., 1986, A&A 165, 135
Rodonò M., Cutispoto G., 1992, A&AS 95, 55
Rodonò M., Cutispoto G., 1994, In: Callaut J.-P. (ed.) VII Cambridge Workshop on Cool Stars, Stellar Systems and the Sun. ASP Conf. Ser., 459
Rodonò M., Lanza A.F., Catalano S., 1995, A&A 176, 267
Rodonò M., Pagano I., Leto G., at al., 1997, In: Donahue R.A., Bookbinder J.A. (eds.) IX Cambridge Workshop on Cool Stars, Stellar Systems and the Sun. ASP Conf. Ser. 154, 1446
Rucinski S.M., 1977, PASP 89, 280
Scaltriti F., Busso M., Ferrari-Toniolo M., et al., 1993a, MNRAS 264, 5
Scaltriti F., Piirola V., Coyne G.V., et al., 1993b, A&AS 102, 343
Strassmeier K.G., Bartus J., Cutispoto G., et al., 1997, A&AS 125,11
Straižys V., Kuriliene G., 1981, Ap&SS 80, 353
van den Oord G.H.J., de Bruyn A.G., 1994, A&A 286, 181
Vogt S.S., 1981a, ApJ 247, 975
Vogt S.S., 1981b, ApJ 250, 327